February 27, 2015
Faculty of Aerospace Engineering
Delft University of Technology

SIMULATION REPORT

WING BOX STRESS ANALYSIS

Group A11
AE3212-II: Simulation, Verification & Validation

Group Members:

Lucas Bolte
Twan Keijzer
Srijith Menon
Boris Mulder
Floris van Steijn
Karlo Rado

Nomenclature

Symbol	Description	Unit
A_m	mean area of the cross section of the cut	$[m^2]$
B_i	i^{th} Boom area	$[m^2]$
c	local chord	$[m]$
c_r	root chord	$[m]$
c_t	tip chord	$[m]$
ϵ_x	x-offset from the shear centre to the half chord line	$[m]$
g	gravitational accaleration	$[\frac{m}{s^2}]$
h_3	distance from engine to x,z-plane	$[m]$
$i = 30 - z$	distance along wing span starting from tip	
I_{xx}	moment of inertia around x	$[m^4]$
I_{xy}	product of inertia	$[m^4]$
I_{yy}	moment of inertia around y	$[m^4]$
λ	Lift load factor	[-]
Λ	half chord sweep	$[^\circ]$
m_e	engine mass	$[kg]$
M_x	moment around the x-axis	$[N \cdot m]$
M_y	moment around the y-axis	$[N \cdot m]$
M_z	moment around the z-axis	$[N \cdot m]$
q	shear flow	$[\frac{N}{m}]$
S_y	shear force in y direction	$[N]$
σ_i	normal stress at boom i	$[\frac{N}{m^2}]$
σ_z	normal stress in z direction	$[\frac{N}{m^2}]$
T_e	engine thrust	$[N]$
t_{bottom}	thickness of the bottom spar	$[m]$
t_{front}	thickness of the front web	$[m]$
t_{rear}	thickness of the rear web	$[m]$
t_{top}	thickness of the top spar	$[m]$
ρ_f	density of the fuel	
τ_{xz}	shear stress in the xz-plane	$[\frac{N}{m^2}]$
τ_{yz}	shear stress in the yz-plane	$[\frac{N}{m^2}]$
V_f	Fuel volume	[L]
W_e	engine weight	$[N]$
$\overline{x}$	x coordinate of the centroid	$[m]$
$\overline{y}$	x coordinate of the centroid	$[m]$
$z = -(i - 30)$	distance along the wingspan starting from root	

Table 0.1:

Chapter 1

Introduction

Airbus just recently introduced the Airbus A350XWB which is a competitor to the Boeing 787 Dreamliner series from the new generation of Airbus and Boeing aircraft. Both aircraft are highly innovative with a composite fuselage and wing structure. To enhance the efficiency of the design of these aircraft both Airbus and Boeing are interested in creating a structural analysis tool to size their wings. The tool should be able to calculate normal and shear stress distributions in a wing box, which result from internal forces and moments due to the applied loading conditions. The results produced have to be verified and validated by data from earlier structural experimental results. The output of the tool will allow for preliminary sizing of the wing box. Even though the developed tool is considered to be a low-fidelity simulation tool which will be only used for preliminary sizing of the wings, it should be as close to reality as possible. In short it can be said that the tool should be able to calculate the shear- and normal stresses in the wing box coming as close to reality as possible.

To keep the program fast and affordable assumptions have to be made. Which assumptions are made and how they will affect the output is discussed in chapter 2. In chapter 2 also the reference frame is defined and the governing equations are presented. Based on the governing equations an analytical solution is presented in chapter 3. This solution will later be used for the verification of the tool. In chapter 4 the numerical solution, which will be the base of the tool, is presented. Chapter 4 also explains the structure of the source code of the tool and presents a flowchart of this structure. Chapter 5 elaborates on the verification of the numerical solution, comparing it to the analytical solution. In Chapter 6 the validation of the numerical solution is discussed. The conclusions, based on the verification and validation can be found in chapter 7. A task division can be found in Appendix A.

Chapter 2

Problem Analysis

It is important that the essence of a problem is clear before it is being solved. To get a solution which is compatible with the objective of the problem a clear problem analysis should be done. The most important part of understanding a problem is knowing which variables/effects shouldn't and which should be taken into account. The assumptions are discussed in section 2.2, where the assumptions and their effects on the solution are stated. In section 2.3 the equations that are used for both analytical and numerical solutions will be explained. The reference frame with respect to which all calculations are to be done is explained and visualised in section 2.4

2.1 Problem statement

The aim of this project was to develop a tool for structural analysis of a wing box. The problem for which the normal- and shear stress have been calculated is Sierra loadcase 1, where the wing box is a tapered rectangular hollow beam as can be seen in figures 2.2 and 2.3. The different loads that are applied on the wing box are depicted in figure 2.1, where the wing is illustrated as a beam clamped at the root. Therein f is the fuel load, mg is the engine weight, $\lambda c(i)$ is the distributed lift loading as a function of i.

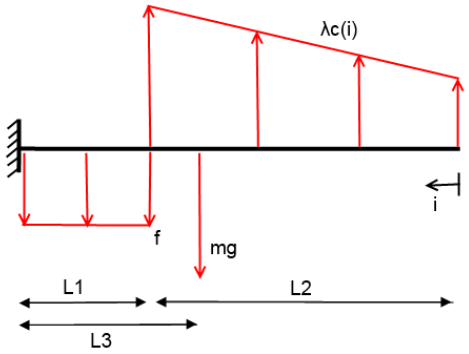

Figure 2.1: Diagram showing all loads acting on the wing box in y-direction

In addition to the loading types illustrated in figure 2.1, there is also a thrust force T_e which acts in the positive x-direction. The location of thrust is at the i position of the engine weight and a h_e distance from the centroid of the beam (with respect to the negative y-direction). These loads eventually lead to the shear and normal stresses in the structure, which are the output variables of the tool. The solution procedure is explained in parts 2.3 and 3.2(for the analytical solution) and 4.2(for the numerical solution).

2.2 Assumptions

Before doing any calculations, the assumptions taht were used have to be stated clearly. In order to judge the validity of these assumptions, the consequences and implications for further analysis have to be known. Assumptions can be divided into primary and secondary assumptions. Primary assumptions have a major impact on the solution whereas secondary assumptions have a minor impact. The primary assumptions are stated first.

- First of all, it is assumed there are no stiffening structures present. Since the problem does not mention any stiffeners, these are not taken into account. This is a primary assumption, since stiffening structures such as stiffeners could make a major impact on the stress analysis results. Especially for bending it could make a significant difference. The assumption is still considered as valid, since the problem does not state stiffeners of any kind.
- It is assumed that the drag of the wing is equal to zero. Since the total drag of the airplane is equal to the total thrust, the total drag could be evaluated. However, the contribution of the wing drag to the total drag is unknown. Therefore it is difficult to evaluate this wing drag. Neglecting the wing drag is a primary assumption, since the order of magnitude of the drag is the same as the order of magnitude of the engine thrust, which is included in the analysis. Leaving the drag on the wing out will lead to a lower shear stress in the x direction and a lower bending moment around the y axis in the part of the wing box where drag is acting. For the torque, it would make a sufficiently small difference whether to leave wing drag out or not.
- The assumption is made that the wing box structure is mass-less. This is assumed in order to simplify the analysis of the wing box structure significantly. However, this is a primary assumption, since the order of magnitude of the mass of the wing will be the same as the order of magnitude of the mass of the engine. This means the results of the analysis could have a major impact. For the shear and bending moment, a wing with mass would counteract the lift distribution, which lowers the shear and bending moment significantly.
- An assumption is made regarding the lift load factor $\lambda(t)$. It is assumed to be constant in time. This means the fuel weight and flight conditions do not change. In a real flight, the fuel weight would change over time, so the load factor would also change. Also flight conditions would be varying due to gusts, climbing, descending and so on. This assumption is primary, since the weight of a wing with maximum fuel loaded differs significantly from a empty wing. Also different flight conditions could change the wing loading by a significant amount. As stated at the assumption above, a heavier wing box would counteract the lift force, inducing a smaller bending moment and shear force.
- An assumption considering the stress concentrations is that there are none. This means no concentrated stresses are present. This is simplifying the structural analysis significantly. This assumption is a primary assumption, since the impact on the results is major in case of a structural weakness.

The secondary assumptions are:

- The height of the engine h_3 is the distance between the neutral axis (axis of symmetry, centre of the wing box), and the point where the thrust acts upon. This is a secondary assumption, since the torque contribution of the thrust is expected to be small, which is the only use of h_e.
- Due to the near symmetry of the structure (where the only asymmetry is the front spar being $5/3$ times as large as the rear spar), the shear centre is assumed to be located at the same point as the centroid. This is a secondary assumption given the dimensions of the structure and the similarities of the thicknesses.
- An assumption regarding the lift load factor λ is that it is assumed to be a uniformly distributed load. This is due to the fact that λ is given to be a singular value.
- It is also assumed that deflections do not cause a change in magnitude and direction of loads acting on the wing box. This is a fundamental structural analysis assumption. If this assumption is not made, an iterative process would follow. Then the direction and magnitude of the load is dependent on the deflection at a certain moment in time, which cause a different magnitude and direction of the load, which continues with an infinite amount of iterations. However, the actual stresses would not differ significantly from the computed stresses, so this assumption is secondary.
- The wing box is assumed to be centered in the middle of the wing, which implies that the wing box starts from the quarter chord to the three quarter chord (from 0.25c to 0.75c). Since many aircraft have the wing box located in the wing in a similar way, this is considered a valid assumption. On top of that, the wing box would only move a quarter chord at most, which is not a significant amount. This assumption creates a minor difference between the calculated torque and the actual torque.
- It is assumed that the loads due to the engine are all point forces. This is a secondary assumption since it implicates no major impacts on the results of the computations. Since the engine is probably suspended to a small area of the wing, its thrust and weight can be modeled as point forces instead of distributed forces.
- The material is assumed to be isotropic, so all properties of the material are identical in all directions. In reality a structure is more or less anisotropic, depending on the production methods used. Still this is a minor and basic structural assumption, since it would not imply impacts on the results of large magnitude.

- The second basic structural assumption made is that of absence of structural imperfections. It means no production or assembly errors are present. This is a secondary assumption, since it implies no major change of the results of the computations.
- The chord length varies linearly with the z direction. This assumption is made, since no information about this is provided.
- The contribution to the moments of inertia of the skin of the wing is neglected. This assumption is reasonably valid, since a thin skin would not be able to bear a significant bending load. The implication of this assumption is that the stresses in the wing box are lower in reality than in the computed results.
- It is assumed that the wing box is clamped at the root. In reality this is almost the case, since the fuselage would actually cause a reaction force and moment. So this assumption comes close to reality.
- For the structural analysis of the wing box, the box is assumed to be thin-walled. This is done in order to simplify calculations. In reality, the moments of inertia would be different of the assumed moments of inertia, and the stresses would vary slightly over the thickness of the walls.
- For the lift, it is assumed that it acts at the quarter chord line. In fact, it would act over the whole surface of the wing, but this assumption implies a significant simplification. The consequences are that in reality the stresses will not exactly be equal to the computed stresses.
- It is assumed that the lift acts parallel to the y-axis, so that there is a 90 degrees angle between the upper or lower panel skin of the wing box and the lift force. This assumption has been made, since a possible deviation of this 90 degrees would be sufficiently small that is has almost no impact on the structural analysis.

2.3 Governing equations

The first step is to find λ, the lift distribution. This was done by dividing the given lift by the area over which half L (the lift over both wings) acts at.

$$\lambda = \frac{L}{2 \cdot L_2(c_r + c_t)/2} = \frac{L}{L_2(c_r + c_t)} \tag{2.1}$$

Where c_r is the root chord, c_t is the tip chord, and L_1, L_2, L_3 can be seen in figure 2.2. The rest of the governing equations used for analytical and numerical will be discussed in section 3.2. The main difference between the analytical and numerical methods is the evaluation of an integration, where the numerical solution transforms it into a summation, as illustrated in equation 4.17.

2.4 Reference Frame

The reference frame used will be Cartesian, where its origin lies on the innermost part of the wing box structure (at root chord) and the centroid of the wing box cross section. The reference frame is illustrated in figure 2.2 and figure 2.3. In figure 2.2, the Y-axis comes out of the paper and in figure 2.3, the Z-axis comes out of the paper. Furthermore, for the analytical solution there is also a coordinate i, as can be seen in 2.1.

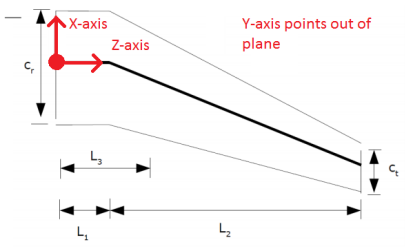

Figure 2.2: Reference frame projected on top view of the wing

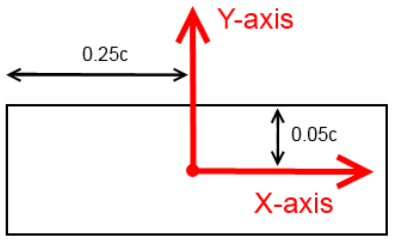

Figure 2.3: Reference frame projected from the side (looking from tip to the root)

Chapter 3

Analytical Solution

The following section deals with the outline of the procedure that will be followed in order to obtain a simplified analytical solution. With regard to this solution additionally made assumptions will be stated and their impact will be discussed with respect to the theory. In section 3.1 additional assumptions that are introduced for the proposed analytical solution are stated. In section 3.2 the solution procedure is explained taking into account the theory elaborated in the section 2.

3.1 Assumptions and definitions

In order to find the normal and shear stresses along the wing box some assumptions have to be made, in addition to the assumptions from section 2.2. The assumption that normal stresses, those produced by bending, are not affected by the taper of the structure. This is a secondary assumption, because if the taper is sufficiently small, then the effect on the normal stresses produced by bending are minimal.[1, p.362] This assumption slightly reduces the accuracy of the analytical solution, but it simplifies the calculations.
The height of the engine h_3 is defined to be the vertical distance from the centroid (which coincides with the reference frame) to the point of action of the thrust force.

3.2 Governing equations and theory

In this section the theory used for calculations will be discussed. Within, all the assumptions and symbolic expressions will be noted, such as to present a clear overview for the calculations and discussion that will follow. In order to analyse the complete wing box, it is divided into three sections:It is important to state that for the analytical solution the analysis has been carried out starting from tip going towards the root. For this transformation the following notation has been used $30 - z = i$. Starting from the tip, section one goes from 0 to $L_1 + L_2 - L_3$. Section two starts at a distance of $L_1 + L_2 - L_3$ and ends at L_2. The last part, section three, is the straight section from L_2 until the root, which is $L_1 + L_2$. Please note, that the notation i denotes the distance from tip towards the root.

Firstly, geometric properties of the wing box are clarified. Secondly, the location of centroid and the moment of inertia are calculated. In the following the constants for the distributed loads are determined and the shear Forces and the resulting moments are completed. After the normal stress analysis has been undertaken, the basic shear flows in the cross section are calculated. Lastly, the shear flows due to an offset to the shear centre are determined and dividing these two added shear flows by the thickness leads to the shear stress.

3.2.1 Geometric properties

The local stresses in the wing box are dependent on the local cross-section of the wing box, which in turn is a function of the chord length. Furthermore, the lift distribution is also a function of chord length. Therefore, the geometrical analysis of the wing box would be the first step. First of all, it is assumed that the chord length is c_t at the tip ($i = 0$), and that it linearly increases from c_t at $i = 0$ to c_r at $i = L_2$, which also denotes the end of section two. This yields to the following equation:

$$c_i = c_t + i \cdot \frac{c_r - c_t}{L_2} \tag{3.1}$$

Where c_i is the local chord length as a function of i. In section three, when $i \leq L_2$ the chord length is assumed to be c_i. , and $u(L_2 - i)$ is a step function that is one up till and including $i = L_2$, and zero after $z = L_2$. This allows us to find the wing box cross-sectional thicknesses:

$$t_{front}(i) = t_{front} \cdot c_i \qquad t_{rear}(i) = t_{rear} \cdot c_i \qquad t_{top}(i) = t_{top} \cdot c_i \qquad t_{bottom}(i) = t_{bottom} \cdot c_i \tag{3.2}$$

Given that the cross-sectional width is $0.5c_i$ and its depth is $0.1c_i$, all desired geometrical properties are obtained.

Centroid and moment of inertia

Assuming thin walls, computation of the centroid of the structure with respect to the local reference frame can be found as follows:

$$\bar{x} = \frac{t_{front}(i) \cdot 0.5c_i \cdot 0.25c_i - t_{rear}(i) \cdot 0.5c_i \cdot 0.05c_i}{t_{rear}(i) \cdot 0.1c_i + t_{top}(i) \cdot 0.5c_i + t_{bottom}(i) \cdot 0.5c_i + t_{front}(i) \cdot 0.1c_i} \tag{3.3}$$

Since each cross section is symmetrical over the x-axis ($t_{top} = t_{bottom}$) the following always holds:

$$\bar{y} = 0 \tag{3.4}$$

Knowing the x- and y- location of the centroid, $\bar{x}$ and $\bar{y}$, as a function of i, the moments of inertia can be found. The thin walled assumption is still applied and the thickness of the top and bottom parts is the same, thus the cross-section is symmetric. Equations for the moments of inertia can be found in Hibbeler [2, p.787, p.791].

$$I_{xx} = \frac{t_{front}(i)(0.1c_i)^3 + t_{rear}(i)(0.1c_i)^3}{12} + 0.5(t_{top}(i) + t_{bottom}(i))c_i(0.05c_i)^2 \tag{3.5}$$

$$I_{xx} = \frac{17}{3} \cdot 10^{-6} \cdot c_i^4 = 5.66667 \cdot 10^{-6} \cdot c_i^4 \tag{3.6}$$

$$I_{yy} = \frac{(t_{top}(i) + t_{bottom}(i))(0.5c_i)^3}{12} + 0.5(t_{top}(i) + t_{bottom}(i))c_i\bar{x}^2 + 0.1t_{rear}(i)c_i(0.25c_i + \bar{x})^2 + 0.1t_{front}(i)c_i(0.25c_i - \bar{x})^2 \tag{3.7}$$

$$I_{yy} = \frac{61}{672} \cdot 10^{-3} \cdot c_i^4 = 0.00273 \cdot c_i^4 \tag{3.8}$$

The only terms in the cross-section's I_{xy} are Steiner terms, since the cross-section of the beam can be subdivided into 4 rectangles, which all have an individual I_{xy} of 0 due to their symmetrical properties:

$$I_{xy} = 0 \tag{3.9}$$

3.2.2 Calculation of the Distributed Loads

In this subsection the calculations of the distributed load factors(fuel weight/m and lift/m^2 are shown).

Distributed Fuel Weight

Since in load case one, the fuel is only located in the inner tank from $i = L_2$ until the root and the chord length is constant in this section, the following equation gives the distributed fuel load factor. Please note $L_1 = 2.88m$.

$$f = \frac{V_f \cdot \rho_f \cdot g}{2 * L_1} = \frac{15000l \cdot 0.81\frac{kg}{l} \cdot 9.81\frac{m}{s^2}}{2 * 2.88m} = 20.693\frac{kN}{m} \tag{3.10}$$

Distributed Lift

There are two point forces, namely the engine weight acting in the negative Y-direction, and the engine thrust acting in the positive X-direction at $i = L_1 + L_2 - L_3$. Furthermore, a distributed lift acts on the quarter chord line of the swept part of the wing in sections one and two (from $i = 0$ until $i = L_2$). In the third section the distributed fuel weight acts on the quarter chord line along the wing span (from $i = L_2$ until $i = L_1 + L_2$). The lift distribution is found through:

$$l(i) = \lambda \cdot c_i \tag{3.11}$$

This equation leads to the following term over the entire wingspan, which produces lift:

$$\frac{MLW \cdot g}{2} = \lambda \cdot \frac{c_t + cr}{2} \cdot L_2 \tag{3.12}$$

$$\lambda = \frac{193 \cdot 10^3 kg \cdot 9.81 \frac{m}{s^2}}{(1.69m + 6.27m) \cdot 2.88m} = 8.74 \frac{kN}{m^2} \tag{3.13}$$

3.2.3 Shear forces

Where $l(i)$ is the distributed lift loading at a certain wing span point. The distributed fuel weight $f(i)$ is constant. This, in combination with the weight and thrust of the engine, yield the shear force at each location in the wing box. The weight of the engine, W_e, is found by multiplying its mass, m_e, with the gravitational acceleration, and the thrust, T_e, is given. The shear forces however, are found per section:

In the first section $(0 \leq i < L_1 + L_2 - L_3)$

$$S_y(i) = \int_0^i l(i')di' = \lambda(\frac{1}{2} \cdot i^2 \cdot \frac{c_r - c_t}{L_2} + c_t \cdot i) \tag{3.14}$$

$$S_x(i) = 0 \tag{3.15}$$

In the second section $(L_1 + L_2 - L_3 \leq i < L_2)$:

$$S_y(i) = \int_0^i l(i')di' - m_e \cdot g = \lambda(\frac{1}{2} \cdot i^2 \cdot \frac{c_r - c_t}{L_2} + c_t \cdot i) - m_e \cdot g \tag{3.16}$$

$$S_x(i) = T_e \tag{3.17}$$

In the third section$(L_2 \leq i < L_1 + L_2)$:

$$S_y(i) = \int_0^{L_2} l(i')di' - m_e \cdot g - \int_{L_2}^i f(i')di' = \lambda(\frac{L_2}{2} \cdot (c_r - c_t) + c_t \cdot L_2) - m_e \cdot g - f(i - L_2) \tag{3.18}$$

$$S_x(i) = T_e \tag{3.19}$$

3.2.4 Bending Moments

The bending moments are caused by the lift, the fuel weight, the engine weight, and the engine thrust and are given in the following corresponding to each section. In the first section $(0 \leq i < L_1 + L_2 - L_3)$

$$M_y(i) = 0 \tag{3.20}$$

$$M_x(i) = \int_0^i S_y(i')di' = \lambda(\frac{1}{2} \cdot i^2 \cdot \frac{c_r - c_t}{L_2} + c_t \cdot i) \tag{3.21}$$

In the second section $(L_1 + L_2 - L_3 \leq i < L_2)$:

$$M_y(i) = \int_{L_1+L_2-L_3}^i S_x(i')di' = T_e \cdot (i - L_1 - L_2 + L_3) \tag{3.22}$$

$$M_x(i) = \int_{L_1+L_2-L_3}^i S_y(i')di' = \lambda(\frac{1}{2} \cdot i^2 \cdot \frac{c_r - c_t}{L_2} + c_t \cdot i) - T_e \cdot (i - L_1 - L_2 + L_3) \tag{3.23}$$

In the third section $(L_2 \leq i < L_1 + L_2)$::

$$M_y(i) = \int_{L_2}^i S_x(i')di' = T_e \cdot (i - L_1 - L_2 + L_3) \tag{3.24}$$

$$M_x(i) = \int_{L_2}^i S_y(i')di' = \lambda(-(\frac{1}{6} \cdot c_t + \frac{1}{3} \cdot c_r) \cdot L_2^2 + \frac{1}{2}(c_r - c_t) \cdot L_2 \cdot i) - m_e \cdot g(i - L_1 - L_2 + L_3) - \frac{1}{2}(i - L_2)^2 \tag{3.25}$$

3.2.5 Normal stresses

The normal stresses in this structure are only generated due to moments. It is assumed that the wing box does not experience any other normal loads. Furthermore, the equation itself assumes some of the assumptions as discussed in 2.2, such as no deflections, and linearly elastic and homogeneous material. In addition to that, it is assumed that the taper does not influence the stresses due to bending moments as discussed in 3.1.

$$\sigma_i(x, y, i) = \frac{M_y I_{xx} - M_x I_{xy}}{I_{yy} I_{xx} - I_{xy}^2} x + \frac{M_x I_{yy} - M_y I_{xy}}{I_{yy} I_{xx} - I_{xy}^2} y \tag{3.26}$$

[1, p.485]. Where x and y are coordinates on the cross-section, and σ_Z is the first output variable, namely the normal stress. All moments are dependent on i. Due to symmetry the equation simplifies to the following:

$$\sigma_i(x, y, i) = \frac{M_y}{I_{yy}} x + \frac{M_x}{I_{xx}} y \tag{3.27}$$

In the different sections, this leads to the following normal stress distributions taking into account the moments of inertia, the moment equations and their parameters such as λ:
In section one:

$$\sigma_i(x, y, i) = \frac{5.39574 \cdot 10^{10} \cdot i^2 (i + 30.1233)}{(i + 10.0441)^4} y \tag{3.28}$$

In section two:

$$\sigma_i(x, y, i) = \frac{5.39574 \cdot 10^{10} \cdot (i^3 + 30.1322 i^2 - 230.771 i + 4684.640)}{(i + 10.0441)^4} y + \frac{8.7965 \cdot 10^{11} (i - 20.3)}{(i + 10.0441)^4} x \tag{3.29}$$

In section three:

$$\sigma_i(x, y, i) = -1.1814 \cdot 10^6 \cdot (i^2 - 140.478 i + 2114.19) y + 456194 \cdot (i - 20.3) x \tag{3.30}$$

The results of this analysis may be found in figure 3.3

3.3 Shear stress analysis

Secondly, the shear forces are needed in order to compute all shear stresses. This means the location of all shear forces have to be known. Then a shear flow can be split up in a basic shear flow and a constant shear flow. Using the shear flow and thicknesses, the shear stresses can be calculated.

3.3.1 Shear stresses

The shear stresses can be computed using the following equation:

$$\tau = \frac{q_s}{t} \tag{3.31}$$

In order to find the shear stresses of a thin-walled closed section beam structure, first the shear flow has to be defined:

$$q_s = q_b + q_{s,0} \tag{3.32}$$

$q_{s,0}$ is the closed section shear, q_b is the basic shear flow (of an open cross-section). q_b can be found using the following equation.

$$q_b = -\frac{S_x I_{xx} - S_y I_{xy}}{I_{xx} I_{yy} - I_{xy}^2} \int_0^s t x ds - \frac{S_y I_{yy} - S_x I_{xy}}{I_{yy} I_{xx} - I_{xy}^2} \int_0^s t y ds \tag{3.33}$$

Since the thicknesses of the top and bottom panel are the same, the cross section has one axis of symmetry, so $I_{xy} = 0$.

In figure 3.1 s starts at point 0, which is in the centre of the rear panel. Now, for all panels, the shear flow can be evaluated. It follows that:

$$q_{b01} = \frac{S_x \cdot t_{rear}}{I_{yy}} (0.25 {c_i}^2 s) - \frac{S_y \cdot t_{rear}}{I_{xx}} (0.5 s^2 c_i) \tag{3.34}$$

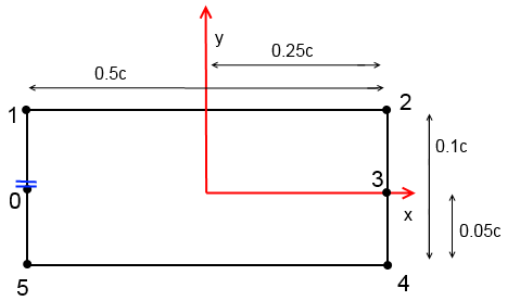

Figure 3.1: Reference frame and distances used for computing the basic shear flow

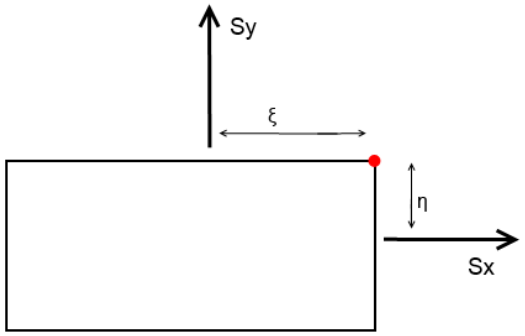

Figure 3.2: The point where moment equivalence has been taken around

$$q_{b12} = -\frac{S_x \cdot t_{top}}{I_{yy}}(0.5s^2c_i - 0.25{c_i}^2 s) + \frac{S_x \cdot t_{rear}}{I_{yy}}(0.0125{c_i}^3) - \frac{S_y \cdot t_{top}}{I_{xx}}(0.05{c_i}^2 s) - \frac{S_y \cdot t_{rear}}{I_{xx}}(0.00125{c_i}^3) \tag{3.35}$$

$$q_{b23} = -\frac{S_x \cdot t_{front}}{I_{yy}}(0.25{c_i}^2 s) + \frac{S_x \cdot t_{rear}}{I_{yy}}(0.0125{c_i}^3) + \frac{S_y \cdot t_{front}}{I_{xx}}(0.5s^2c_i - 0.05{c_i}^2 s) - \frac{S_y \cdot t_{top}}{I_{xx}}(0.025{c_i}^3) - \frac{S_y \cdot t_{rear}}{I_{xx}}(0.00125{c_i}^3) \tag{3.36}$$

$$q_{b34} = \frac{S_x \cdot t_{rear}}{I_{yy}}(0.25{c_i}^2 s) - \frac{S_x \cdot t_{front}}{I_{yy}}(0.0125{c_i}^3) + \frac{S_x \cdot t_{rear}}{I_{yy}}(0.0125{c_i}^3) + \frac{S_y \cdot t_{front}}{I_{xx}}(0.5s^2c_i) - \frac{S_y \cdot t_{front}}{I_{xx}}(0.00125{c_i}^3 - \frac{S_y \cdot t_{top}}{I_{xx}}(0.025{c_i}^3 - \frac{S_y \cdot t_{rear}}{I_{xx}}(0.00125{c_i}^3) \tag{3.37}$$

$$q_{b45} = \frac{S_x \cdot t_{bottom}}{I_{yy}}(-0.5s^2c_i + 0.25{c_i}^2 s) + \frac{S_x \cdot t_{rear}}{I_{rear}}(0.0125{c_i}^3) - \frac{S_y \cdot t_{bottom}}{I_{xx}}(0.05{c_i}^2 s) - \frac{S_y \cdot t_{top}}{I_{xx}}(0.025{c_i}^3) - \frac{S_y \cdot t_{rear}}{I_{xx}}(0.00125{c_i}^3) \tag{3.38}$$

$$q_{b50} = \frac{S_x \cdot t_{rear}}{I_{yy}}(-0.25{c_i}^2 s + 0.0125{c_i}^3) \tag{3.39}$$

In these expression, t_{bottom} and t_{top} are interchangeable, since these values are equal. Now the constant shear flow $q_{s,0}$ has to be evaluated per section. This is done using the equation from Megson [1, p.514].

$$S_x\eta - S_y\xi = \oint pq_b ds + q_{s,0} \tag{3.40}$$

This equation is a moment equivalence equation. For this, the shear forces are needed. These are already evaluated in the section shear force 3.3. This moment equivalence is taken about a point in the cross section.

This calculation uses the point which is in the top right corner of the wing box. For this the distances η and ξ have to be evaluated. For the contribution of S_y by the lift, the distance to the top right corner is evaluated as:

$$\xi_L = \frac{0.5c_t i + \frac{1}{6L_2}(c_r - c_t)i^2}{c_t + \frac{1}{2L_2}(c_r - c_t)i} \cdot \tan(\Lambda_0.25c) \tag{3.41}$$

This expression for ξ_L depends on i. Since every shear force (so for example due to the lift or due to the weight of the engine) has its own distance to the top right corner, there are different expressions for every contribution.

Secondly, the closed integral of the shear flow times the distance has to be evaluated. All shear flows in every section have been computed already. Using these, the following can be computed:

$$\oint pq_b ds = \frac{S_x}{I_{yy}}(-\frac{1}{960}{c_i}^5 t_{bottom} - \frac{1}{1600}{c_i}^5 t_{rear}) + \frac{S_y}{I_{xx}}(\frac{1}{1600}{c_i}^5 t_{top} + \frac{1}{16000}{c_i}^5 t_{rear}) \tag{3.42}$$

Finally, the moment equivalence equation can be made for three sections. By filling in the expression for $\oint pq_b ds$ and rewriting, the expression for $q_{s,0}$ can be found. For $0 < i < L_1 + L_2 - L_3$:

$$-\lambda(0.5c_t i^2 + \frac{1}{6L_2}(c_r - c_t)i^3) \cdot tan(\Lambda_{0.25c}) = \oint pq_b ds + 2Aq_{s,0} \tag{3.43}$$

$$q_{s,0} = -\frac{\lambda}{0.1{c_i}^2}((0.5c_t i^2 + \frac{1}{6L_2}((c_r - c_t)i^3)tan(\Lambda_{0.25c}) + (c_t i + \frac{1}{2L_2}(c_r - c_t)i^2) \cdot (\frac{3750}{34}(c_i t_{top} + \frac{375}{34}c_i t_{rear})))) \tag{3.44}$$

For $L_1 + L_2 - L_3 < i < L_2$:

$$(m_e g(i - L_1 - L_2 + L_3) - \lambda(0.5c_t i^2 + \frac{1}{L_2}(c_r - c_t)i^3))tan(\Lambda_{0.25c}) + T_e(h_3 + 0.05c_i) = \oint pq_b ds + 2Aq_{s,0} \tag{3.45}$$

$$\begin{aligned} q_{s,0} = \frac{1}{0.1{c_i}^2}((m_e g(i - L_1 - L_2 + L_3) - \lambda(0.5c_t i^2 + \frac{1}{L_2}(c_r - c_t)i^3))tan(\Lambda_{0.25c}) \\ +T_e(h_3 + 0.05c_i + \frac{700}{61}c_i t_{top} + \frac{420}{61}c_i t_{rear})) + (m_e g - \lambda c_i)(\frac{3750}{34}c_i t_{top} + \frac{375}{34}c_i t_{rear}) \end{aligned} \tag{3.46}$$

For $L_2 < 0 < L_1 + L_2$:

$$\begin{aligned} m_e g((L_3 - L_1)tan(\Lambda_{0.25c}) - \lambda(0.5c_t {L_2}^2 + \frac{1}{6}(c_r - c_t){L_2}^2)tan(\lambda_{0.25c}) \\ +T_e(h_3 + 0.05c_t) + 0.25f(i - L_2)c_r = \oint pq_b ds + 2Aq_{s,0} \end{aligned} \tag{3.47}$$

$$\begin{aligned} q_{s,0} = \frac{1}{0.1{c_i}^2}(m_e g(L_3 - L_1)tan(\Lambda_{0.25c}) - \lambda(0.5c_t {L_2}^2 + \frac{1}{6}(c_r - c_t){L_2}^2)tan(\lambda_{0.25c}) + T_e(h_3 + 0.05c_t) \\ +0.25f(i - L_2)c_r + (m_e g + f(i - L_2) - 0.5\lambda(c_r + c_t)L_2) \cdot (\frac{3750}{34}c_r t_{top} + \frac{375}{34}c_r t_{rear}) + T_e(\frac{700}{61}c_r t_{top} + \frac{420}{61}c_r t_{rear})) \end{aligned} \tag{3.48}$$

In these equations $c_i = c_t + \frac{c_r - c_t}{L_2}i$.

Now, the q_b on every section is evaluated and the $q_{s,0}$ too. So the total shear flow can be found. Therefore, the shear stresses can be found according to the following formula:

$$\tau = \frac{q_b + q_{s,0}}{t} \tag{3.49}$$

Here, t is the thickness of the specific panel. The results of this analysis may be found in figure 3.3

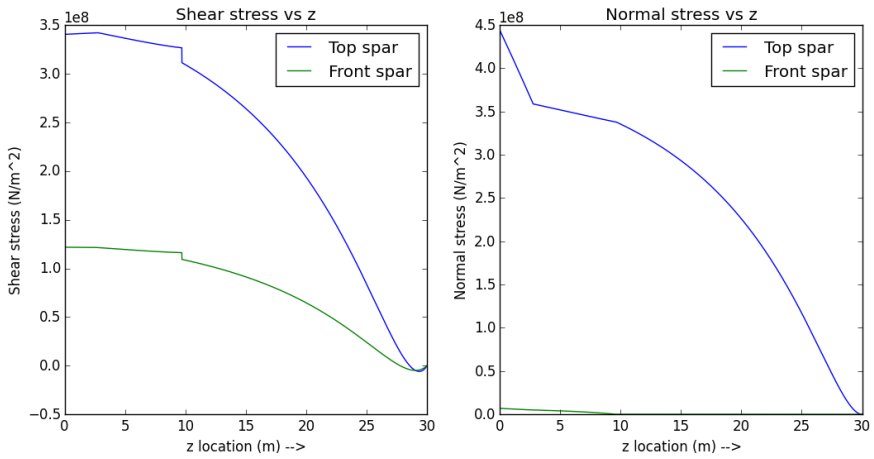

Figure 3.3: Graph showing the analytical solutions for the stress distributions with respect to z=-(i-30)

Chapter 4

Numerical Solution

After the analytical solution is done, the numerical solution should be obtained. A python program is written which calculates the normal and shear stresses along the spars in the wingbox. In section 4.1 of this section the assumptions that are used, are explained. In section 4.2 the equations used in the Python program are shown and explained. In section 4.3 the modules of the code are explained and in section 4.4 is shown.

4.1 Assumptions for the Numerical Solution and its impact

The numerical solution is meant to resemble the reality as accurate as possible. The analytical solution is used to evaluate the validity of the numerical solution. Therefore in the analytical solution some more assumptions can be made than in the numerical solution. This section explains all the assumptions used.

Firstly, no assumptions regarding taper have to be made, since the numerical method consists of n parts, each having a constant local chord length.

Secondly, the stresses in the wing box are calculated by splitting it op in tiny section which give a small numerical calculation error due to the fact that the chord is taken to be constant along this small section. This is a secondary assumption added for the numerical solution. Because the size of these sections is very small, the error induced by this will also be small.

Thirdly, for all function that need to be integrated there is a small error due to the fact that these function are also cut up into small sections. Therefore, the area of this section is not exactly the same as the size underneath the actual graph. This also induces minor errors to the solution.

4.2 Governing equations for the numerical solution

First the chord length at a specific point along the span of the wing (local chord) has to be calculated. The Lift and the size of the wing box are dependent on the local chord. Equation 4.1 can be used to calculate the local chord.

$$\begin{cases} z < l_1 & c = c \\ z >= l_1 & c = c_t + (c_r - c_t)\frac{l_1+l_2-z}{l_2} \end{cases} \tag{4.1}$$

When the chord is known the centroid is needed to be able to calculate the moment of inertia. Equations 4.2 and 4.3 are used for this.

$$\overline{x} = \frac{\sum_{i=1}^{4} A_i \cdot x_i}{\sum_{i=1}^{4} A_i} \tag{4.2}$$

$$\overline{y} = \frac{\sum_{i=1}^{4} A_i \cdot y_i}{\sum_{i=1}^{4} A_i} \tag{4.3}$$

With the center of gravity known the moments of inertia can be calculated with equations 4.4, 4.5 and 4.6. As can be seen in equation 4.5 only the Steiner term counts for I_xy, due to symmetry of all webs and spars separately.

$$I_{xx} = \sum_{i=1}^{4} (\frac{1}{12} b_i h_i^3 + y_i^2 A_i) \tag{4.4}$$

$$I_{xy} = \sum_{i=1}^{4} (x_i y_i A_i) \tag{4.5}$$

$$I_{yy} = \sum_{i=1}^{4} (\frac{1}{12} b_i^3 h_i + x_i^2 A_i) \tag{4.6}$$

To be able to calculate the shear force acting on a certain cross-section first the weight of the engine and the lift force at the local point along the span are needed. These can be obtained with equations 4.7 and 4.8.

$$L = \lambda_l c \tag{4.7}$$

$$W_e = m_e g \tag{4.8}$$

Now the shear force y direction can be determined according to equations 4.9.

$$\begin{cases} z < l_1 & S_y = L + W_e + W_f \\ l_1 < z < l_3 & S_y = \int_z^{l_1+l_2} L \; dz + W_e \\ l_3 < z < l_1 + l_2 & S_y = \int_z^{l_1+l_2} L \; dz \end{cases} \tag{4.9}$$

Also, the shear force in x direction, which is created due to the engine, can be calculated with equation 4.10.

$$\begin{cases} z > l_3 & S_x = 0 \\ l_1 < z < l_3 & S_x = T_e \end{cases} \tag{4.10}$$

With these S_x and S_y the moments on the wing can be calculated with equation 4.11 and 4.12

$$M_y = \int_z^{l_1+l_2} S_x \; dz \tag{4.11}$$

$$M_x = \int_z^{l_1+l_2} S_y \tag{4.12}$$

Now the moments in the wing are known, the normal stresses can be obtained from this. This can be done using equation 3.26.

With the shear forces calculated earlier the shear center, and after that the shear flow can be calculated. Two fictional forces are applied to the assumed shear center at (ϵ_0, η_0). The real location of the shear center is to be calculated later. The open section shear stress can than be calculated with equation 4.13. This equation has to be applied on each four sides of the wing box separately.

$$q_b = -\frac{I_{xx}S_x - I_{xy}S_y}{I_{xx}I_{yy} - I_{xy}^2} \int_0^s tx \; ds - \frac{I_{yy}S_y - I_{xy}S_x}{I_{yy}I_{xx} - I_{xy}^2} \int_0^s ty \; dsq \tag{4.13}$$

Integrating the open section shear and dividing by the length of the component you intefate over yields $q_{s,0}$. This is done in equation 4.14.

$$q_{s,0} = -\frac{\oint q_b \; ds}{\oint \; ds} \tag{4.14}$$

Taking moments around any (smartly chosen) point yields equation 4.15. This gives the shear center coordinates.

$$S_x\eta_0 - S_y\epsilon_0 = \oint q_s p \; ds + 2Aq_{s,0} \tag{4.15}$$

The open section shear flow can be found by filling in equation 4.13 with the actual shear force. though, this shear force should first be moved to act through the shear center, which creates a torque. Together with the torque from the Lift, the Weight of the engine and the trust this are the total external torques. The stress from these torques can be calculated using equation 4.16.

$$q_{s,0} = \frac{T_{ex}}{2A} \tag{4.16}$$

Additionally there is a shear stress that bridges the difference between an open and a closed section. This stress can be calculated using equation 4.14. Adding these three stresses up yields the total shear stress.

All integrating equations will be calculated with a numerical integrating algorithm as shown in equation 4.17.

$$\int_a^b f(x)dx = \sum_{n=a}^{N \cdot h} f(n) \cdot h \tag{4.17}$$

Where f(x) is the function to be integrated, h the step size and $N = \frac{b}{h}$.

4.3 Explanation of Code Modules

Centroid: The centroid of a section along the wingbox is calculated from the thicknesses of the the spars which in their case are a function of the chord length.
Chord Length: The chord length is calculated in two ways depending on the desired section along the wingbox. From the root to l_1 the chord length is constant while from l_1 to l_2 the chord decreases from the root chord length to the tip chord length.
Engine Weight: The engine weight unit calculates the shear force induced by the engine at a certain z location.
Fuel Weight: The fuel weight unit calculates the shear force fuel weight on a specific z location in the wing.
Moment of Inertia: In order to compute the moment of inertia, the dimensions of the wingbox are put into a 4 by 2 matrix and the x and y coordinates were placed into arrays. Once this is done, the moments of inertia in the x and y axis are computed using the functions produced earlier.
Lift: The lift unit calculates the moment caused by the lift.
Shear Force and Moment: The shear force is calculated by adding all forces from tip to root. This shear force graph is integrated to get to the moments. This units calculate the shear force and moment in section z along the wingspan.
Torque: The torque on a certain section due to lift and the engine is calculated in this unit. The forces are moved to the centroid and therefore a torque needs to be added to compensate for this. The torque unit outputs this torque on given section z.
Shear Flow: From the computations of the Moments of Inertia and all shear forces, the variable shear flow qb could be determined first. From where the computation begins, the shear flow is set to zero and then calculated for each side of the wingbox using the correct coordinates and dimensions. Once this variable shear flow has been computed, the results are placed in arrays for further use and the constant shear flow qso is computed next and added to the variable shear flow to calculate the total shear flow for the wingbox. Once this is done, the results are plotted for visual understanding and examination.
Normal Stresses: The normal stresses were a function of the moment of inertias, the moments and the distances from the neutral axis. The normal stresses were put into a matrix and was left for validation against experimental data.
Shear Stresses: The shear stress computation was fairly simple, since most of the coding was made for the shear flows. The shear stress was a function of the shear flow and the different wingbox thicknesses. So for, each side of the wingbox, the corresponding shear stresses were computed along the wingspan.

4.4 flowchart

The flowchart depicts the processes in the program and their interconnections.

4.5 Results

By combining all modules and by using all equations mentioned in this chapter values for the normal stress and shear stress have been calculated. The maximum values found in each cross section have been plotted in figures 4.2 and 4.3.

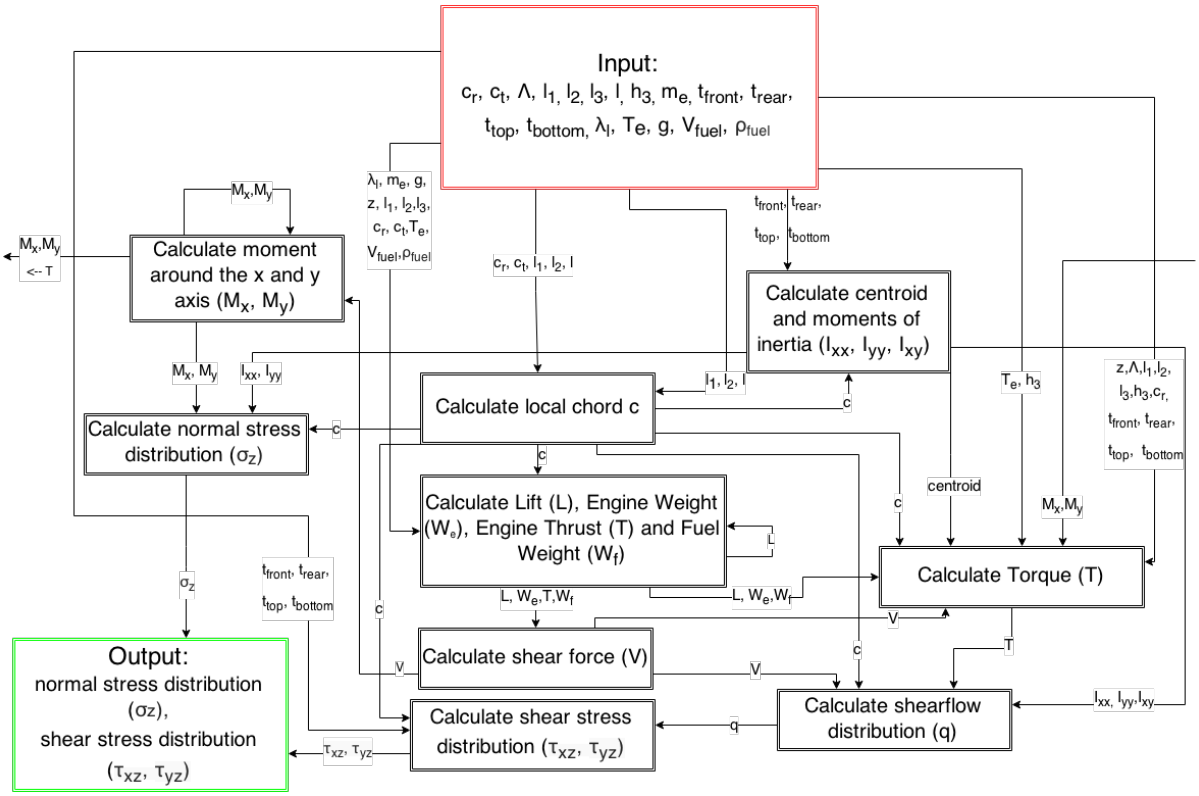

Figure 4.1: flowchart describing the data flows and modules in the program

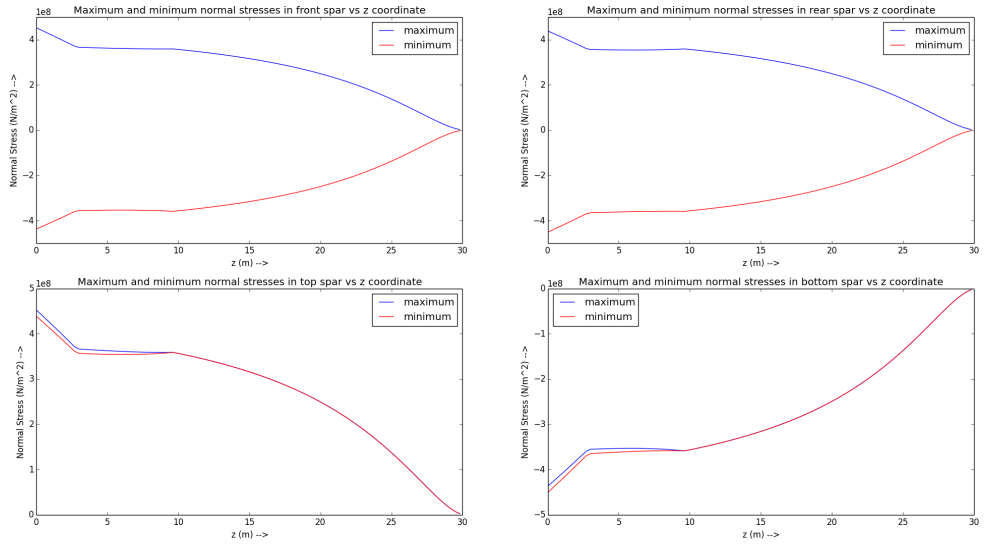

Figure 4.2: maximum normal stress distribution over the wingspan

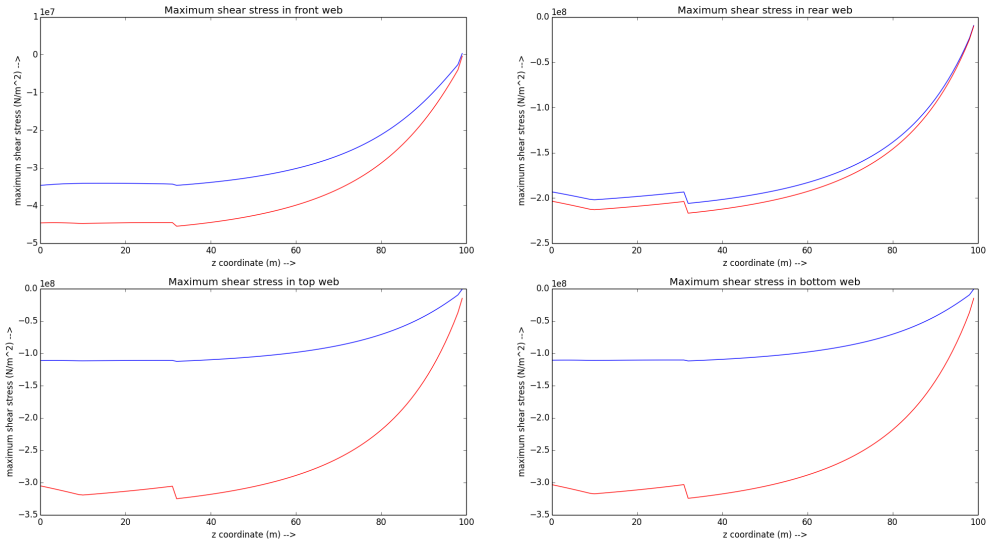

Figure 4.3: maximum Shear stress distribution over the wingspan

Chapter 5

Verification

The main goal of the verification process is to spot flaws in the simulation and to check whether or not the program functions properly. In order to make the simulation program as accurate as possible, it is necessary to include a verification process. One way of doing that is by plotting graphs, which will give a good impression and idea if the results are accurate. Secondly, one compares the results of basic analytical equations with the results of the simulation program. It is recommended to verify data in a range of different locations in the structure. Since the simulation is performed using Python programming, the simulation is separated into individual modules. The verification of the simulation program can be done using two steps. First the individual code modules are checked after which the simulation is verified against a simpler case against the analytical solutions of the stresses produced in the wingbox beam. In this section the verification method of individual code modules is explained. Because the simulation program was programmed with individual codes, unit testing is easier. A main Python code was implemented to call all the other codes to run and output the shear and normal stresses that can simulate the wingbox structural analysis tool.

5.1 Verification of Individual Code Modules

Analytical and numerical values are compared for four different locations along the length of the beam. The first location will be at the root of the wing, the second is at length 'L_1' , the third is where the engine is located and the final location is at the tip of the wing. It is believed that these locations are enough for the verification of the modules to the analytical equations as it provides a good insight into how the simulation works for the critical points on the wing. The modules that will be verified are the moment of inertia, the shear flows, the shear stresses and the normal stresses. The verification of these modules can make sure that all other modules will be correct since every other parameter is used in the calculation of these modules. Each module was assigned unit tests to do a quick verification and sort out bugs and syntax errors. This implementation of unit tests greatly sped up the process of verification and allowed for efficiency when sorting out issues with the numerical model.

Verification of Moments of Inertia

Location along Beam Length	Analytical Solution	Numerical Solution
Root Chord	0.008757 m^4	0.008651 m^4
Chord at L_1	0.008757 m^4	0.008651 m^4
Chord at Engine	0.003916 m^4	0.003876 m^4
Chord at Tip	0.0000462 m^4	0.0000446 m^4

Table 5.1: Moment of Inertia Ixx

From the results obtained here, it is understood that the simulation is running according to the analytical equations for this particular case at least. There is a slight difference in the values, but that is believed to be the thin-walled assumption in the analytical solution as well as round-off errors.

Verification of Normal Stresses

From the data collected, it can be understood that the normal stresses computed correspond to the values given by the analytical equations. Hence this module is also verified for this case.

Location along Beam Length	Analytical Solution	Numerical Solution
at Root	455 MPa	449 MPa
at L_1	359 MPa	355 MPa
at Engine	373 MPa	369 MPa
at Tip	0 MPa	0 MPa

Table 5.2: Maximum Normal Stresses in the Front Spar

Verification of Shear Stresses

Location along Beam Length	Analytical Solution - MAX	Numerical Solution - MAX
at Root	-105 MPa	-102 MPa
at L_1	-104 MPa	-99 MPa
at Engine	-108 MPa	-101 MPa
at Tip	0 MPa	-0.06 MPa

Table 5.3: Shear Stresses in the Top Panel

In the tables provided, the data shows the Moment of Inertia (Ixx), Maximum occuring Normal Stresses and Maximum occuring Shear Stresses with varying wingspan length. The data was computed and verified with the analytical equations for four different points on the wingbox. This is only part of the data portrayed in the tables as the other modules were verified in a similar manner but cannot be put up due to page restrictions. The verification process revealed that the underlying analytical solutions matched the simulation computations for various points on the wing hence, proving that the simulation can be used as a valid structural analysis tool. From the data collected, it can be understood that the shear stresses computed, correspond to the values given by the analytical equations. Hence this module is also verified for this case. This was not the case initially. A lot of verifying for this module was done before results were obtained. The shear flows, moments and centroid modules were also verified separately just as these few other modules were tested and compared to the analytical results. The data cannot be provided here due to the restriction of pages of content in the report.

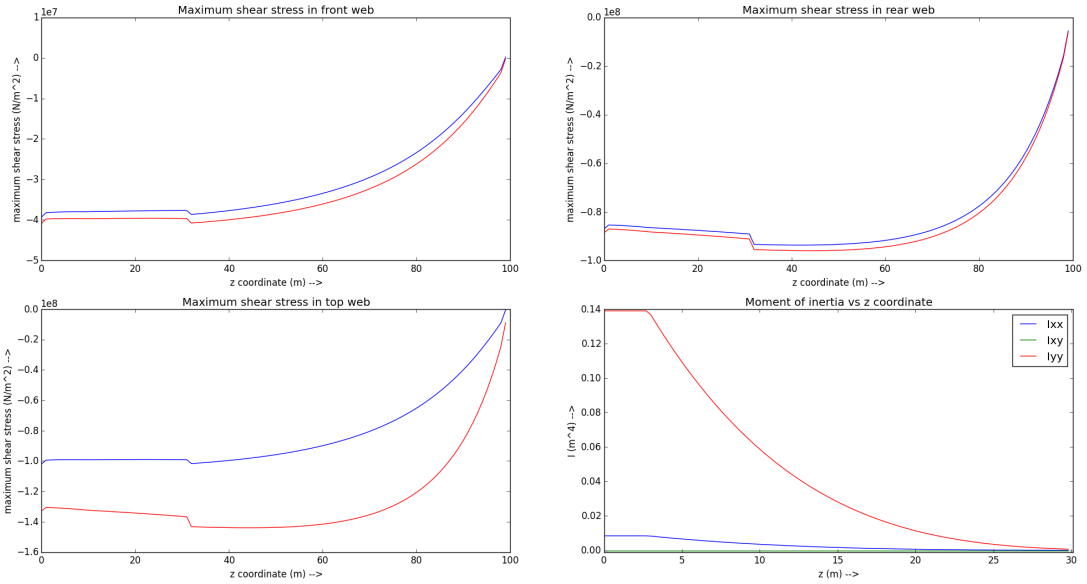

Figure 5.1: Shear Stress Distribution along wing

5.2 Verification of the full model with a simplified problem

Besides verifying every code module separately the complete simulation tool is also to be verified by introducing a simplified problem. This would translate to determining the stresses and forces acting on the beam with simpler geometry and less complexities. The introduction of a simplified problem is mainly a quick check for whether or not the output of (more complex) variables of the simulation are of the same order of magnitude and have the correct sign. Strong deviations in the output with a simpler model may imply that the tool has in fact a few errors and must therefore be revised further before use. It is expected that the simplified problem will have a more constant stress distribution and lower stresses due to the absence of wing sweep.

Assumptions for simplifying the problem were constant thicknesses of all the wing box sides, no sweep angle and a constant chord length, which implies there is no taper. For the thickness, the average thickness was taken to be 2mm and the root chord length was used for all calculations.Verification of the individual modules pointed out that the majority of the simulation produced results that were confirmed by analytical solutions. It is expected that the simplified problem will have a more constant stress distribution and lower stresses due to the absence of wing sweep.

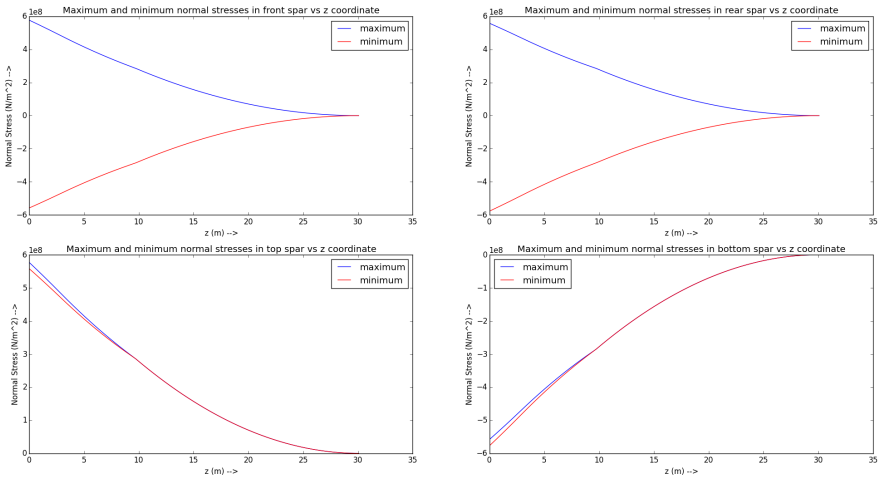

Figure 5.2: Normal Stress Distribution with simplified problem

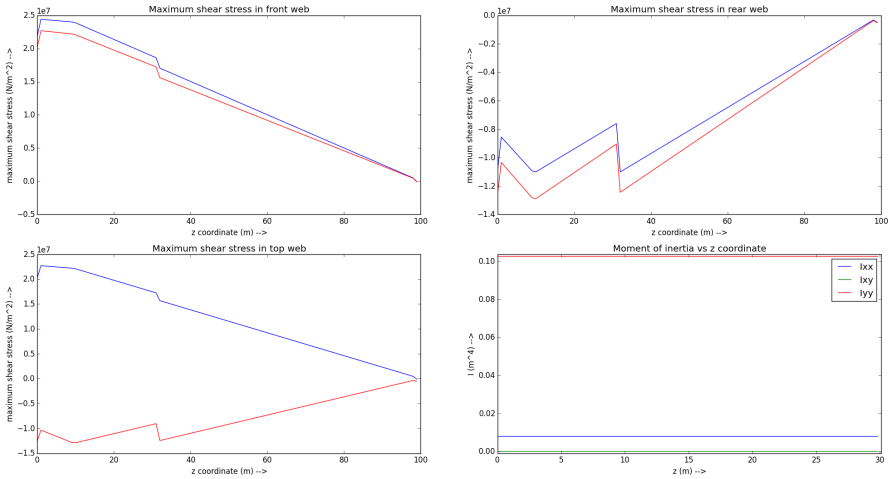

Figure 5.3: Shear Stress ditribution with simplified problem

5.3 Verification Results

Verification of the individual code modules pointed out that there were minor deviations from the analytical equations but they were mainly caused due to rounding off errors. The major source of concern was the computation of the shear flows and shear stresses effectively. The initial program was greatly deviating from the analytical solutions and the program was constantly debugged and updated in order to compute the shear flows accurately and efficiently. After multiple unit tests, verification and modifications, the shear stress distribution was verified to be accurate to the analytical solutions. Every other individual module ran smoothly but due to the inaccuracy in the shear stress distribution, the computed Von Mises stresses were also inaccurate.

In the simplified model we could see that the simulation was able to compute the required stresses and modify itself to the varying parameters that would allow in the design phase of the wing. The fact that the results correspond to the analytical solutions explains that the simulation is working properly and implies that the need for revision, or rather fine-tuning the simulation tool will be minimal. This is provided that the underlying analytical equations used, can be validated from the experimental data later during the validation process. Nonetheless, it is believed that the numerical computation of the basic shear flow varies slightly with the analytical equations for the basic shear flow which is mainly what brings about the differences.

In the verification of the full model with a simplified problem, it could be seen that the results produced for the normal stresses followed a different curve compared to the given conditions. This can be explained by the fact that the thicknesses were kept constant throughout the wing box for this particular case. With the loading type remaining the same, this would change the stresses and stress development along the wing box as many other parameters such as moments, moment of inertia and the wing box dimensions have to be factored. The same can be said about the shear stress distribution.

From all these conclusions and explanations, it can be said that the numerical model is moderately verified to be able to simulate the structural stresses within the wing box.

Chapter 6

Validation

In order to conclude whether the simulation can be used to accurately predict the behaviour of a wingbox beam, validating its results with experimental data is mandatory. Furthermore, the validation process can be used as an input for iteration and improvement of the current simulation output. In this chapter the validation of the von mises stresses will be covered, as well as the differences and recommended improvements of the simulation.

6.1 Validation of the full model

The main purpose of this chapter is to explain the process and the conclusions drawn during the validation of the simulation model to the experimental data provided. In order to compare the results, the von mises stresses were compared along the length of the wingbox. It is important to bear in mind that the axis system used in the experimental data is different to the system used in the numerical simulation. To be able to understand whether or not the simulation data was accurate enough to the test data, the simulated shear and normal stresses had to be converted to von mises stresses.

6.2 Comparison of the Test Data with the Numerical Model

As can be seen from the graph, the numerical solution does manage to model the experimental data. There are a few areas to inspect nonetheless. The graph can be split into two areas for inspection. Just like the front end of the wing, the error difference in stresses on the top panel between the numerical analysis and test data is of the order between 15 to 25 percent. But in this case this is a larger deviation, where the difference can be translated between 90MPa-100MPa

6.2.1 Front skin analysis

First, the front section of the wing and the top panel. In the front of the wing, the numerical analysis is a better estimate than the analytical solution in modelling the actual stresses experienced by the wing. The analytical solutions are believed to be correct considering it predicts the curve of the experimental data and since the numerical solutions are based off the analytical solutions, the numerical solutions do predict the magnitude of the average von mises stresses even though they are off slightly. The average experimental data at the front show that the stresses are constant mostly throughout the wingspan except for one area where there is a large peak. This area of stress concentration after inspection is believed to be where the engine lies. This could be the reason why there might be a peak in the von mises stresses. When inspecting this area further other than the stress peak observed at the engine, the simulation comes to within a difference in range of 20-30 MPa from the actual test data. This can be translated to an error ranging between 15 to 25 percent. Even though this isnt the accuracy that was expected, it can be understood that an estimation around and about 20MPa is very good. The errors near the root of the span, will be discussed in section 6.2.2.

6.2.2 Top skin analysis

Just like the front end of the wing, the error difference in stresses on the top panel between the numerical analysis and test data is of the order between 15 to 25 percent. But in this case this is a larger deviation, where the difference can be translated between 90-100MPa. Aside from the two large discrepancies on the tip and root of the validation data, the numerical solution constantly overestimates the validation data. This can be best linked to coding errors, which result in a false shear flow. The analytical solution more closely models the numerical data, and the slight, but constant, offset can be explained by epimistic uncertainties in material properties or production. There is another offset in the analytical calculation, however, which is located at

the engine point. This could be a mistake in torque calculation due to thrust.
Near the tip chord in the top average of the validation data, there is a sudden increase in stress. According to our model there are no normal stresses in the z-direction that could explain a non-zero stress at the tip of the wing. This could either be due to wing vortices inducing a torque or local normal stresses which were assumed not be present, or sensor data errors which is not dependent on the model.
Furthermore, there is another large discrepancy near the root chord of the engine which starts at 4m distance from the root up till the root itself. The sudden decrease at 4m could be explained by a spar which contains the fuel within the inner fuel tank. A spar would decrease the shear stress at its location, but it does not explain the sudden increase. This could be due to the assumption that the beam is simply clamped at the root ($z = 0$), while in reality it could have various internal loadings induced by the fuselage as it is non-simply clamped.

6.3 Simulation Improvements and Recommendations

From thorough analysis the tool seems to be able to model the stresses within the wingbox under a particular loading. The idea is to keep modifying and improving the model to come as close to simulating the actual structural loads on the wing as possible. The numerical model could have a much more sophisticate verification process for the shear flow calculations as it is believed that is what brings about a majority of the deviation from test data. The calculation of the shear center would need to be done extensively as it is believed to be a major factor in the stress calculations. The factor of time has been an issue throughout and more time would definitely allow th model to be fine tuned further and more efficiently. Perhaps choosing a different numerical analysis method such as a finite element method would be helpful, but that would require more time. All in all the the simulation tool does model the stresses experienced by the wingbox for multiple loading scenarios but with further enhancing and modification of the tool, a better and more accurate tool could be developed.

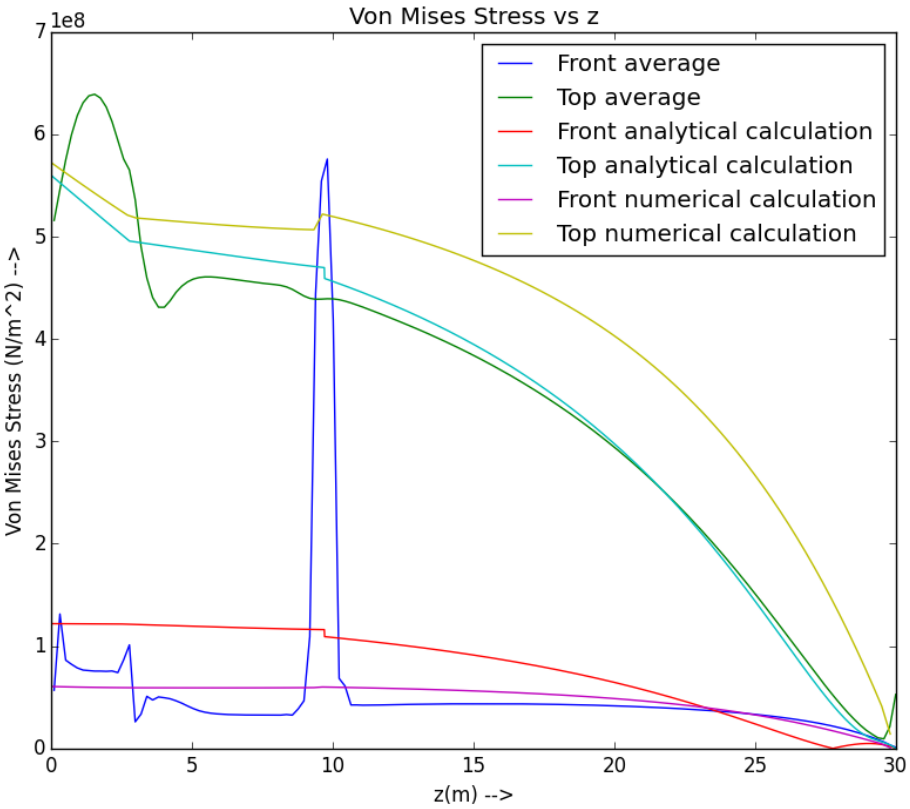

Figure 6.1: Plot of numerical and analytical solution together with the validation data

Chapter 7

Conclusion

In order to produce a low-fidelity tool for preliminary sizing of the wing box, assumptions had to be made. These assumptions generally cause a deviation between the output of the tool and the experimental validation data. Using the validation data, a few findings have been made.

Firstly, a difference between the basic shear flows of the numerical and analytical solutions is clearly visible. However, a major difference between the validation data and the analytical solution is not found. This could imply that an error has been made in computing the q_b using the numerical method. This presumption is supported by the fact that the unit test for the basic shear flow showed that the numerical method for computing the q_b is not valid.

Although a major difference between the analytical solution and validation data could not be found, there is still a difference. This difference is caused in first place by the governing assumptions. These assumptions simplified the computation of stresses, but most likely enlarge the difference between the analytically obtained data and the experimentally obtained validation data. However, there could always be some minor calculation and evaluation errors which could remain unnoticed. Checking calculations even more should decrease these errors.

For the normal stress part, the deviation between the graphs of the numerical and analytical solution is small. Still, there is a deviation, which should be explained by assumptions and errors. For example, the difference in the thin-walled assumption could partly explain the difference in graphs. The numerical normal stress solution is not based on a thin-walled assumption, whereas the analytical solution uses the thin-walled assumption. However, this assumption can only generate a very minor difference between the two graphs, since the thicknesses of the wing box panels are much smaller than the chord lengths. So minor calculation errors still better explain the deviation in the two graphs.

The low-fidelity wing box stress tool should be able to compute normal and shear stresses using a simplified model. This simplification is due to all assumptions. Although the assumptions are responsible for deviation between the numerical solution and the experimental data, if these assumptions are known, they can be taken into account. Most important is, no errors can be made in computing all stresses. Making no computational errors requires more time. Therefore, in the future, the structural analysis tool will need to be evaluated further.

Bibliography

[1] T.H.G Megson. *Aircraft Structures for Engineering Students*. Elsevier, 2007.

[2] R.C. Hibbeler. *Mechanics of Materials*. Prentice Hall, 2011.

Appendix A

Group Organisation

The project spanned a total of 3 weeks, where the simulation planning phase counted for 1 week, and the remainder of the project involved the actual modelling of a structural analysis tool. The work packages involved can be found A.2 along with a Gantt chart showing time allocated to each task in figure A.3 and a work package distribution in A.1.

	Student	Twan Keijzer	Lucas Bolte	Srijith Menon	Karlo Rado	Floris van Steijn	Boris Mulder
Work package	Time (h)						
WP1 - Writing Simulation Plan	30	5	5	5	5	5	5
WP2 - Analytical solution	25		5	4	8	8	
WP3 - Numerical solution	35	12	5	6			12
WP4 - Verification	20	3	3	3	4	4	3
WP5 - Validation	20	3	3	3	4	4	3
WP6 - Reporting	25	4	4	5	4	4	4
WP7 - Quality check	12	1	3	2	3	2	1
Total time (h)	167	28	28	28	28	27	28

Figure A.1: Table showing which team members contributed to each part of the project

Task	Work Package	Start Date	Duration	End Date
Writing Simulation Plan	WP1	10-2-2015	2	12-2-2015
Analytical solution	WP2	16-2-2015	5	21-2-2015
Numerical solution	WP3	16-2-2015	7	23-2-2015
Verification	WP4	21-2-2015	4	25-2-2015
Validation	WP5	23-2-2015	3	26-2-2015
Reporting	WP6	23-2-2015	3	26-2-2015
Quality check	WP7	25-2-2015	1	26-2-2015

Figure A.2: Table showing duration and period of each component of the project

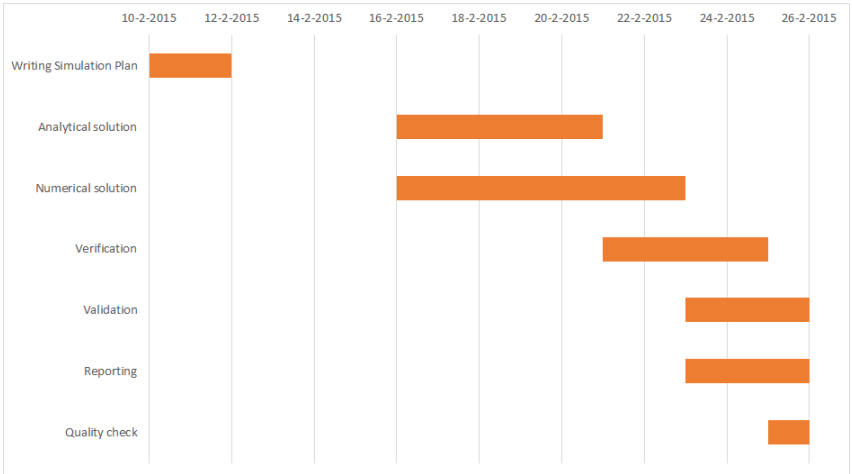

Figure A.3: Graph showing duration and period of each component of the project